GA–A24373

OBSERVATION AND CHARACTERIZATION OF RADIALLY-SHEARED ZONAL FLOWS IN DIII–D

by
G.R. McKEE, R.J. FONCK, M. JAKUBOWSKI,
K.H. BURRELL, K. HALLATSCHEK, R.A. MOYER, W. NEVINS,
D.L. RUDAKOV, and X. XU

JUNE 2003

DISCLAIMER

GA–A24373

OBSERVATION AND CHARACTERIZATION OF RADIALLY-SHEARED ZONAL FLOWS IN DIII–D

by
G.R. McKEE,* R.J. FONCK,* M. JAKUBOWSKI,*
K.H. BURRELL, K. HALLATSCHEK,† R.A. MOYER,‡ W. NEVINS,#
D.L. RUDAKOV,‡ and X. XU†

This is a preprint of an invited paper to be presented at the 30th European Physical Society Conference on Controlled Fusion and Plasma Physics, St Petersburg, Russia, July 7–11, 2003 and to be published in *Plasma Physics and Controlled Fusion.*

*University of Wisconsin, Madison, Wisconsin.
†Institut für PlasmaPhysik, Garching, Germany.
‡University of California, San Diego, California.
#Lawrence Livermore National Laboratory, Livermore, California.

Work supported by
the U.S. Department of Energy
under Contract Nos. DE-FG02-89ER53296, DE-FG03-95ER54294,
DE-AC03-99ER54463 and W-7405-ENG-48

GENERAL ATOMICS PROJECT 30033
JUNE 2003

ABSTRACT

Zonal flows, thought crucial to the saturation and self-regulation of turbulence and turbulent transport in magnetically-confined plasmas, have been observed and characterized in the edge region of DIII-D plasmas. These flows exhibit temperature scaling characteristics and spatial features predicted for geodesic acoustic modes (GAMs), a class of higher-frequency zonal flows seen in nonlinear simulations of plasma turbulence. The zonal flows (GAMs) have been observed in the turbulence flow-field in the radial region $0.85 \leq r/a \leq 1.0$ via application of time-delay-estimation techniques to two-dimensional measurements of density fluctuations, obtained with beam emission spectroscopy (BES). Spatial and temporal analysis of the resulting flow-field demonstrates the existence of a coherent oscillation (approximately 15 kHz) in the poloidal flow of density fluctuations that has a long poloidal wavelength, possibly m=0, narrow radial extent ($k_r \rho_i < 0.2$), and a frequency that varies monotonically with the local temperature. The approximate effective shearing rate, dv_θ/dr, of the flow is of the same order of magnitude as the measured nonlinear decorrelation rate of the turbulence. These characteristics are consistent with predicted features of zonal flows, specifically identified as geodesic acoustic modes, observed in 3-D Braginskii simulations of core/edge turbulence.

1. ROLE OF ZONAL FLOWS IN TURBULENCE SATURATION

Understanding the fully saturated state of turbulence in a magnetically confined plasma is crucial to determining the turbulent-driven cross-field particle and energy transport. Turbulence-driven poloidal flows are believed to be a critical saturation mechanism for plasma turbulence [1–3]. Such zonal flows are predicted to be generated by the turbulence itself through the Reynolds Stress [4], and in turn act to regulate and control the magnitude, radial correlation length, and phase relationship between the density and potential fluctuations, and thus the level of turbulent transport, through nonlinear feedback mechanisms. Zonal flows are radially localized, electrostatic potential structures that are toroidally and azimuthally symmetric (m=0, n=0) and act to regulate the turbulence through time-varying $E \times B$ shear flows, similar to the shear flow suppression of turbulence resulting from equilibrium $E \times B$ shear [5,6]. They may be classified into two general categories, one a low frequency residual flow [2], and the other a higher frequency branch identified as geodesic acoustic modes (GAM) [7–9]

The GAM is an electrostatic acoustic oscillation that results from the non-uniform $\mathbf{E} \times \mathbf{B}/B^2$ flow on a magnetic flux surface in toroidal plasmas. This flow in turn causes an m=1 pressure perturbation ($p \sim p_o \sin\theta$) and an associated radial diamagnetic current that tends to short out the radial electric field. This results in a restoring force that creates a coherent oscillation along the geodesic curve of the flux surface, perpendicular to the magnetic field. The frequency is given approximately as $\omega_{GAM} \approx c_s/R_{major}$ with c_s the local sound speed $\left[c_s = \sqrt{(T_e + T_i)/M_i}\right]$ and R_{major} the major radius of the toroidal device. The actual frequency is modified by factors of order unity that depend on the plasma cross-sectional geometry, T_e/T_I and other parameters.

Despite extensive theoretical work on the role of zonal flows in turbulence saturation, and simulations that predict the existence of such flows [10], little definitive experimental evidence for the existence of zonal flows in high temperature tokamak plasmas has been obtained. Some signatures of zonal flows have been inferred from various measurements in several devices [11-17]. Directly diagnosing zonal flows has proved challenging [18]. Perhaps the most direct method would require a toroidal and poloidal array of high-frequency electrostatic potential measurements in the hot plasma interior. And since any density perturbation associated with zonal flows is expected to be quite small ($\tilde{n}/n|_{ZF} \ll e\tilde{\phi}/T_e|_{ZF}$), direct measurement using more prevalent density fluctuation diagnostics would appear challenging.

An alternative method is to examine the flow field of the density fluctuations using the turbulence imaging capabilities of the beam emission spectroscopy (BES) [19,20]. Zonal flows are expected to act on the turbulence through time-varying radially localized $E\times B$ flows. Figure 1 illustrates the structure of a zonal flow as it relates to this

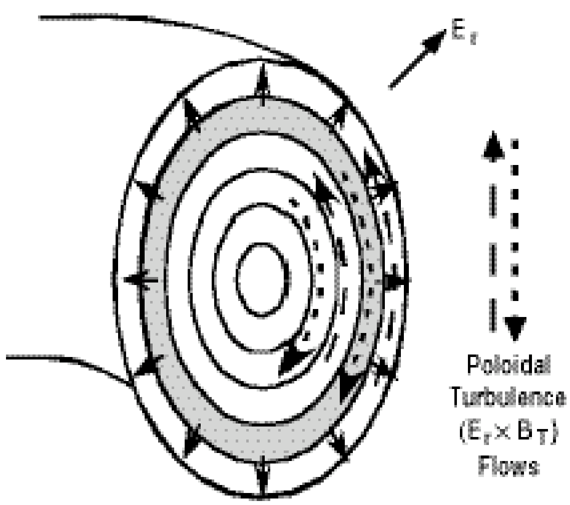

Fig. 1. Conceptual picture of a zonal flow, a radially localized, poloidally and azimuthally symmetric (m=0, n=0) electrostatic potential structure, along with its resulting radial electric field, and E¥B flow. The poloidal E¥B flow of the turbulent eddies is the experimentally accessible feature.

measurement concept. The radially localized electrostatic potential of a zonal flow is indicated by the shaded toroidal annular region, with the associated radial electric field indicated by arrows (solid lines). The resulting poloidal $E_r \times B_T$ flow is shown by arrows (dashed lines). This $E \times B$ flow should contribute to the observable flow of turbulent eddies. A time-varying $E \times B$ flow (such as that resulting from a zonal flow) should thus manifest itself as a modulation of the poloidal flow velocity of the turbulent eddies.

The concept and the methods of analyzing the two-dimensional data are discussed in the next section, followed by a discussion of the results and a summary. This paper presents an overview of the method and central results and the reader is referred to other publications for additional details [21,22].

2. TURBULENCE IMAGING AND FLOW ANALYSIS METHODS

Multipoint measurements of local density fluctuations are utilized to determine the time-dependent turbulence flow field, and thereby to search for evidence of zonal flows. These measurements have been obtained with the beam emission spectroscopy diagnostic at DIII-D [23] which measures local, long wavelength ($k_{\perp}\rho_i < 1$) density fluctuations [24]. The diagnostic measures the Doppler-shifted D_{α} emission (λ = 652–655 nm) from a 75 kV heating neutral beam at 1 μs time resolution [25] and with a spatial resolution of near 1 cm in the radial and poloidal direction. Alignment of the optical sightline-neutral beam intersection volume to a local magnetic field line provides good spatial resolution. Figure 2 indicates the deployment of the 32 available spatial channels relative to the

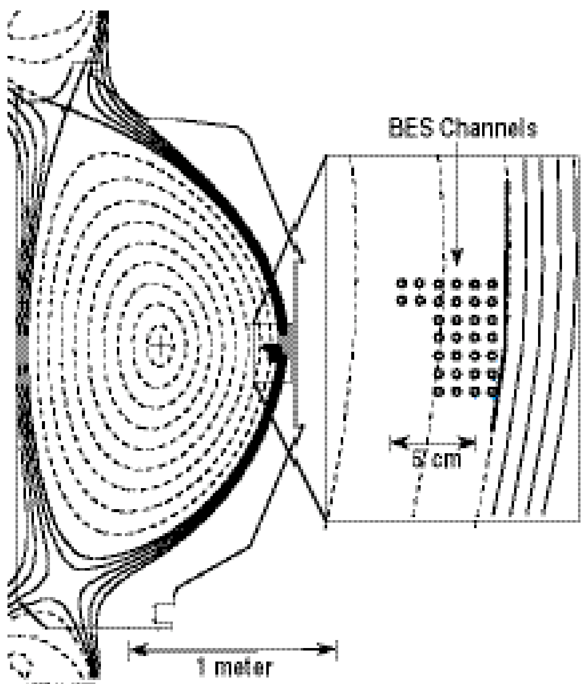

Fig. 2. Deployment of 32 spatial channels of the beam emission spectroscopy system on DIII-D for these experiments. Analysis of the time-resolved two-dimensional data allows for a measurement of $v_q(R, Z, t)$.

magnetic equilibrium for this experiment. An array of 4×7 channels in the radial-poloidal plane (with an additional 2×2 array inside), provides measurements in the region $0.80 < r/a < 1.05$ at the outer midplane. These measurements allow for time-resolved images and movies of the turbulence to be obtained, so long as the turbulence is of sufficient amplitude (approx. $\tilde{n}/n > 5\%$).

Measurement of the time-resolved turbulence flow field has required development of new and modified time-delay-estimation (TDE) analysis techniques [20,26–28]. Zonal flows are expected to be manifest as fluctuations to the poloidal velocity and so TDE methods are applied to poloidally separated density fluctuation measurements. A quasi-static poloidal turbulence flow is typically present and results from a combination of equilibrium $E \times B$ and diamagnetic flows. This velocity is measured by calculating the ensemble-averaged time-lag cross-correlation between two spatially-separated measurements, in this case, $v_\theta = \Delta Z/\tau_{peak}$ with ΔZ the poloidal separation and τ_{peak} the peak of the cross-correlation [29]. In the edge regions of DIII-D plasmas, this equilibrium poloidal turbulence velocity is typically a few km/sec, though varies strongly with radius. It should be noted that this is not the same as the poloidal rotation of the bulk plasma, though the quantities are related through the radial electric field. Zonal flows are thus expected to be manifest as a perturbation on this equilibrium velocity, measurement of which requires the development of high-frequency TDE methods.

Two TDE techniques have been developed and applied for this purpose. One method is a wavelet-based technique that calculates the time-resolved complex wavelet cross-spectrum [26]. The time-resolved time-delay is deduced from the phase of this wavelet cross-spectrum. A thorough characterization of the transfer function relating the measured (output) time-delay to the actual (input) time-delay has been performed using simulations that mimic actual turbulence characteristics [30]. These transfer functions are highly dependent on the underlying density fluctuation spectrum, the amplitude and spectrum of the time-delay itself, and noise inherent in the fluctuation measurements. Calculation of the transfer function thus requires an iterative solution that is performed on a case-by-case basis. The frequency response of this wavelet-based method can extend up to the upper-limits of the underlying density fluctuation spectrum itself, and can be a significant fraction of the Nyquist frequency.

A second technique calculates the time-resolved cross-correlation in the time domain by convolving a narrow time window through a pair of poloidally-separated channels. The time-lag cross-correlation is calculated at each point in time while recording the peak cross-correlation as a function of time [20,27]. It is typically found that reasonable results are obtained using a 20-point time-window, yielding a maximum frequency resolution of one tenth of the Nyquist frequency. The two techniques yield similar results when applied to relatively low-frequency phenomena such as the flows to be investigated here. The wavelet technique yields significantly higher time-resolution, while the time-domain provides greater sensitivity at low frequencies. The transfer functions for the two techniques are shown in Fig. 3, along with the underlying density spectrum used for the

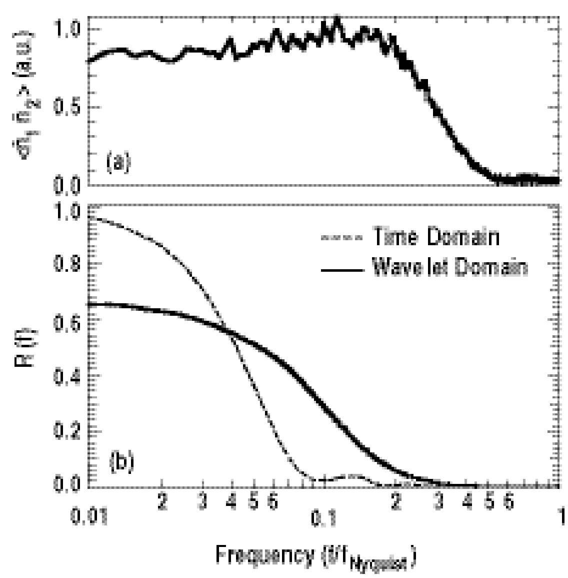

Fig. 3. (a) Measured broadband density fluctuation spectrum for near-edge turbulence, (b) transfer function for the time-resolved cross-correlation (time-domain) and wavelet time-delay-estimation analysis measurements for realistic parameters.

calculations, illustrating the different frequency response and sensitivity of these complementary TDE methods.

3. CHARACTERISTICS OF OBSERVED ZONAL FLOWS

The turbulence flow field, measured via application of the above TDE analysis techniques to spatially-resolved density fluctuation data, reveals features that are consistent with expected characteristics of zonal flows. In Fig. 4, the unprocessed results

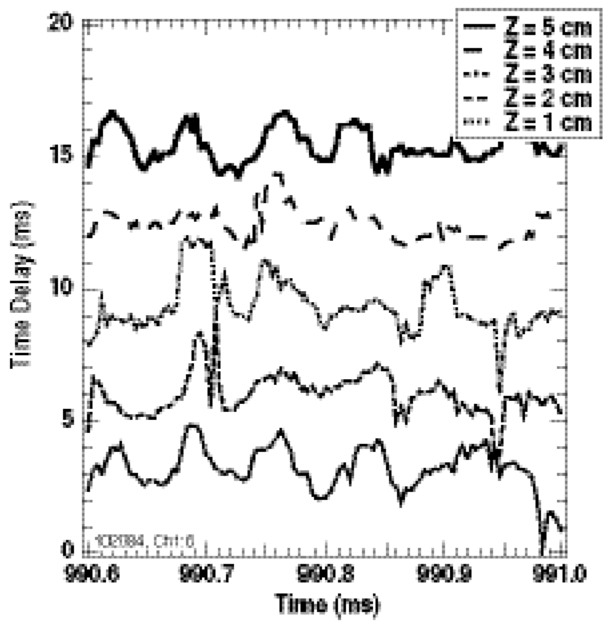

Fig. 4. Example measurements of channel-to-channel time delay; for Z = 1 cm, measurement is in absolute units; for Z = 2–5, measurements are offset by 3 ms/each for visualization. Sinusoidal oscillation of similar amplitude and phase is observed for all measurements.

of the TDE calculation for an array of poloidal measurements are shown. Six channels have been used, and so five adjacent pairs are available. The time-delay measurements for the five pairs in a 400 μs window show remarkable similarities (measurements are offset vertically by 3 μs each for clarity). All show an average of about 3 μs time-delay (~3.3 km/s flow) with an approximately sinusoidal perturbation superimposed. The oscillation has an amplitude of about 25%–40% of the equilibrium value, a period of about 70 μs, and all oscillations appear in phase. The poloidal correlation length of the density turbulence is typically about 3 cm, while these measurements are obtained over a 5 cm domain. Thus although the underlying turbulence itself is largely decorrelated over the spatial domain shown, the derived flow measurements are quite similar.

Spectral analysis of the poloidal turbulence flow measurements from a similar set of discharges is shown in Fig. 5, which shows a clear poloidal flow oscillation near 15 kHz.

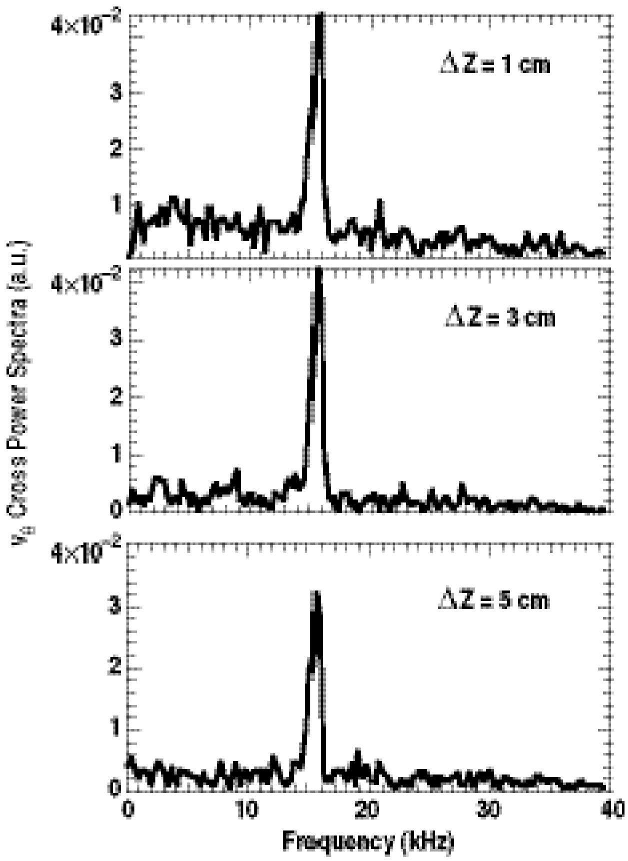

Fig. 5. Cross power spectrum of poloidally separated measurements of $v_q(t)$ indicating a coherent poloidal flow oscillation with high spatial and spectral coherence and long poloidal wavelength.

Here the cross power between the individual flow measurements is measured at increasing poloidal separation and ensemble averaged over 100 ms. Over a distance of 1-5 cm, the oscillation exhibits high spatial and spectral coherence. The poloidal correlation length of this flow pattern is clearly much larger than the 5 cm span of the spatial measurement, and thus much larger than the turbulence correlation length. The narrow spectral width of $f/\Delta f \sim 15$ suggests a long-lived flow structure with a correlation time of at least several hundred microseconds, much longer than the turbulence decorrelation time (typically, $\tau_c \sim 10\ \mu s$).

The poloidal flow oscillation is observed over the entire two-dimensional spatial domain of the imaged density fluctuations (Fig. 1). The phase relationship of the 15 kHz oscillation over the spatially separated measurements is shown in Fig. 6 and demonstrates

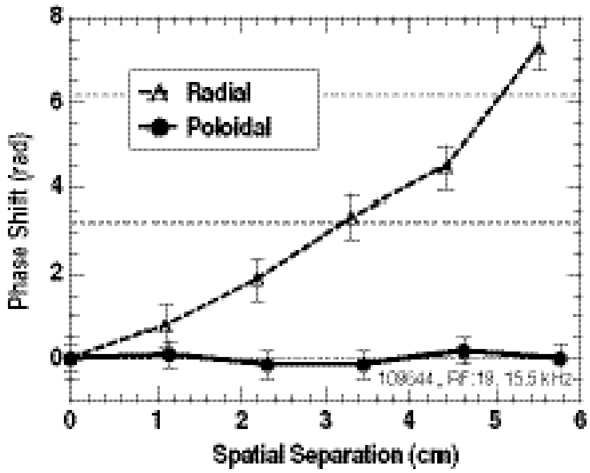

Fig. 6. Phase relation as a function of radial and poloidal separation for the array as shown in Fig. 2. Reference measurement is taken in the corner of the array. Velocity oscillation exhibits little or no measurable poloidal phase shift, but significant radial phase shift which gives rise to a flow shear.

a dramatic spatial asymmetry. Poloidally, there is little or no measurable phase shift of the coherent oscillation, while radially it undergoes a full 180 degree phase shift over a few cm. This suggests a low-m poloidal structure. Error analysis indicates that if a poloidally uniform structure of the form $v = v_o \sin(m\theta)$ is assumed, the poloidal mode number is in the range $|m| < 3$, consistent of course with m=0. The rapid radial phase shift indicates a strong radial shear, dv_θ/dr. that may affect the underlying turbulence. Furthermore, in contrast to the long poloidal correlation of this structure, radially, it has a correlation length of only a few cm [21].

The observed characteristics of this flow oscillation, including its long poloidal wavelength, possibly m=0, coherent frequency, and a frequency close to c_s/R, suggest that this is a GAM, the higher frequency class of zonal flows discussed earlier. To test this hypothesis, the frequency of the flow oscillation was measured as a function of local plasma temperature. The frequency of a GAM is predicted to scale with the local sound speed and thus with temperature. The temperature scan was achieved by varying the input power into the plasma, as well as by examining several time slices within a given discharge (temperature tends to increase with time during the non-equilibrium phase of the discharge). The mode frequency as a function of temperature is shown in Fig. 7. Over

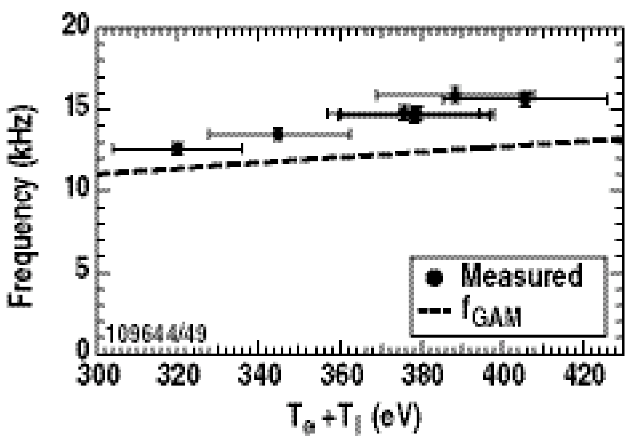

Fig. 7. Frequency of the velocity oscillation as a function of local (electron plus ion) temperature, indicating a dependence of mode frequency on sound speed (note suppressed zero on temperature axis).

several observations, the mode frequency increases monotonically with temperature and scales closely with the predicted GAM frequency, indicated by a dashed line. Recall that the theoretically predicted frequency, $\omega_{GAM} \approx c_s/R_{major}$, has modification terms of order unity, so the 10%–20% deviation between measured and calculated frequencies is not unexpected. These results show remarkable consistency with measurements of a zonal flow structure obtained on the TEXT tokamak with the heavy-ion beam probe (HIBP)

[31,32]. This suggests that the same mode was being observed with a different diagnostic in a different plasma device, indicating a certain universality to the phenomenon.

The magnitude of the poloidal shearing rate [33–35] resulting from the GAM-like velocity oscillation has been estimated using the measured parameters of the flow oscillation [21,22]. The oscillation magnitude is near 0.5 km/s and has a radial wavelength of roughly 6 cm. This translates to a maximum shearing rate of about $\gamma_s \approx dv_\theta/dr \approx 0.3 \times 10^5\ s^{-1}$. Here it is assumed that since the velocity oscillation frequency of 15 kHz is low compared to the bulk of the turbulence spectrum (f < 250 kHz), the effective shearing rate [36] is comparable to dv_θ/dr. The measured nonlinear decorrelation rate of the turbulence is about $1/\tau_c \approx 1 \times 10^5\ s^{-1}$ and thus of comparable magnitude. The flow shearing rate is potentially of sufficient magnitude to affect the turbulence, though not suppress it completely. Indeed, given the relatively large amplitude of the ambient density fluctuations from which the flow was measured, any shear is clearly not suppressing the turbulence.

It was reported that the amplitude of higher frequency density fluctuations ($100 \le f \le 200$ kHz) was modulated at the frequency of the velocity oscillation [22]. It has subsequently been suggested that this apparent oscillation may result from the Doppler-shift of the velocity oscillation itself modulating the frequency of the turbulence spectrum into and out of the fixed frequency spectral window [37]. The amplitude modulation of the density fluctuations is indeed in phase with the velocity oscillation, suggesting that this is a reasonable explanation for the observation. It is also conceivable theoretically that the amplitude modulation should be in phase with the velocity oscillation. Determination of whether the GAM-like velocity oscillation directly modulates the underlying turbulence amplitude will require further examination.

It is noted that the GAM-like coherent poloidal velocity oscillations are not observed in all discharges. Figure 8 shows the coherency spectra of poloidally-separated

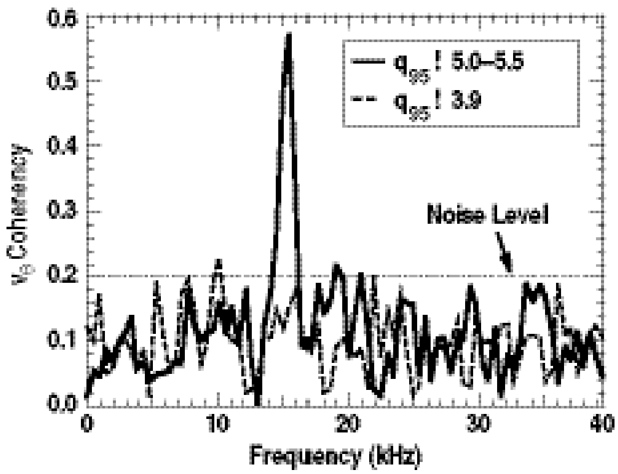

Fig. 8. Coherency of poloidally separated measurements under high q95 and lower q95 conditions. At high q95, the velocity oscillation is readily observed, yet is not apparent at lower q95.

measurements of v_θ in two separate discharge conditions. The mode is readily apparent in one data set, yet is not observed in the second. The plasma parameters and turbulence characteristics are generally similar, with the exception of the edge safety factor, q_{95}. The plasmas with lower q_{95} exhibited no hint of the GAM-like oscillation. This correlation with q_{95} was observed in several sets of discharges obtained over different time periods. This indirectly suggests an inverse dependence of the GAM oscillation amplitude on q_{95}. It will be necessary to perform a systematic scan of q_{95} in otherwise similar discharges to critically test this hypothesis. This study will be left to a future experimental campaign. This inverse dependence on safety factor is at least qualitatively consistent with estimates of the damping rate of GAMs given as $\gamma_{damp} \approx \omega_{GAM} \exp(-q^2)$ [3].

4. SUMMARY

The time-resolved poloidal flow velocity of turbulence has been examined by applying time-delay-estimation techniques to spatially and temporally resolved two-dimensional density fluctuation data obtained with beam emission spectroscopy on DIII-D. The flow field exhibits clear signatures of zonal flows. These features include a coherent poloidal velocity oscillation near 15 kHz with a poloidal mode number of $|m| < 3$ (possibly m=0), and radial localization with a radial wavenumber of near 1 cm^{-1} and radial correlation length of about 2–3 cm. The mode frequency scales with the local sound speed approximately as $f_{v,\theta} \approx c_s/2\pi R$. The inferred shearing rate of this oscillation is comparable to the measured nonlinear decorrelation rate of the turbulence, suggesting that the oscillation is of sufficient amplitude to affect the underlying turbulence. These features suggest that the observed oscillation is a GAM, a class of higher-frequency zonal flows that have been predicted theoretically and are observed in simulations of edge and core turbulence.

REFERENCES

[1] P.H. Diamond, M.N. Rosenbluth, F.L. Hinton, *et al.*, Proceedings of the 17th IAEA Fusion Energy Conference, Yokohama, Japan, 1998 (International Atomic Energy Agency, Vienna, 1999) IAEA-CN-69/TH3/1.

[2] M.N. Rosenbluth, F.L. Hinton, Phys. Rev. Lett. **80**, 724 (1998).

[3] F.L. Hinton, M.N. Rosenbluth, Plasma Phys. Control. Fusion **41**, A653 (1999).

[4] P.H. Diamond, Y.B. Kim, Phys. Fluids B **3**, 1626 (1991).

[5] K.H. Burrell, Phys. Plasmas **4**, 1499 (1997).

[6] K.H. Burrell, Science **281**, 1816 (1998).

[7] N. Winsor, J.L. Johnson, J.M. Dawson, Phys. Fluids **11**, 2448 (1968).

[8] K. Hallatschek, D. Biskamp, Phys. Rev. Lett. **86**, 1223 (2001).

[9] M. Ramisch, U. Stroth, S. Niedner, B. Scott, New J. Phys. **5**, 12.1 (2003).

[10] Z. Lin, T.S. Hahm, W.W. Lee, *et al.*, Science **281**, 1835 (1998).

[11] S. Coda, M. Porkolab, K.H. Burrell, Phys. Rev. Lett. **86**, 4835 (2001).

[12] P.H. Diamond, M.N. Rosenbluth, E. Sanchez, *et al.*, Phys. Rev. Lett. **84**, 4842 (2000).

[13] G.R. Tynan, R.A. Moyer, M.J. Burin, C. Holland, Phys. Plasmas **8**, 2691 (2001).

[14] R.A. Moyer, G.R. Tynan, C. Holland, M.J. Burin, Phys. Rev. Lett. **87**, 135001-1 (2001).

[15] Y.H. Xu, C.X. Yu, J.R. Luo, *et al.*, Phys. Rev. Lett. **84**, 3867 (2000).

[16] M.G. Shats, W.M. Solomon, Phys. Rev. Lett. **88**, 045001-1 (2002).

[17] G.S. Xu, B.N. Wan, M. Song, Phys. Plasmas **9**, 150 (2002).

[18] T.S. Hahm, K.H. Burrell, Z. Lin, *et al.*, Plasma Phys. Control. Fusion **42**, A205 (2000).

[19] C. Fenzi, R.J. Fonck, M. Jakubowski, G.R. McKee, Rev. Sci. Instrum. **72**, 968 (2001).

[20] G.R. McKee, C. Fenzi, R.J. Fonck, M. Jakubowski, Rev. Sci. Instrum. **74**, 2014 (2003).

[21] M. Jakubowski, R.J. Fonck, G.R. McKee, Phys. Rev. Lett. **89**, 265003 (2002).

[22] G.R. McKee, R.J. Fonck, M. Jakubowski, *et al.*, Phys. Plasmas **10**, 1712 (2003).

[23] G.R. McKee, R. Ashley, R. Durst, R.J. Fonck, *et al.*, Rev. Sci. Instrum. **70**, 913 (1999).

[24] R.J. Fonck, P.A. Dupperex, S.F. Paul, Rev. Sci. Instrum. **61**, 3487 (1990).

[25] R.J. Fonck, R. Ashley, R. Durst, *et al.*, Rev. Sci. Instrum. **63**, 4924 (1992).

[26] M. Jakubowski, R.J. Fonck, C. Fenzi, G.R. McKee, Rev. Sci. Instrum.**72**, 996 (2001).

[27] H.C. So, Electron. Lett. **34**, 722 (1998).

[28] C. Hidalgo, M.A. Pedrosa, B. Goncalves, New J. Phys., **4**, 51.1 (2002).

[29] R.D. Durst, R.J. Fonck, G. Cosby, H. Evensen, Rev. Sci. Instrum. **63**, 4907 (1992).

[30] M. Jakubowski, Ph.D Thesis, University of Wisconsin-Madison (2003).

[31] P. Schoch, "Experimental evidence of zonal flows using HIBP data," Bull. Am. Phys. Soc. **47**, 298 (2002).

[32] P.M. Schoch, K.A. Connor, D.R. Demers, X. Zhang, Rev. Sci. Instrum. **74**, 1846 (2003).

[33] H. Biglari, P.H. Diamond, P.W. Terry, Phys. Fluids B **2**, 1 (1990).

[34] T.S. Hahm, K.H. Burrell, Phys. Plasmas **2**, 1648 (1995).

[35] P.W. Terry, Rev. Mod. Phys. **72**, 109 (2000).

[36] T.S. Hahm, M.A. Beer, Z. Lin, *et al.*, Phys. Plasmas **6**, 922 (1999).

[37] P.M. Schoch, Personal communication (2003).

ACKNOWLEDGMENT

This is a report of work supported by the U.S. Department of Energy under Grant Nos. DE-FG02-89ER53296 and DE-FG03-95ER54294 and Contract Nos. De-AC03-99ER54463 and W-7405-ENG-48.